

# Cosmology and Astrophysics of Minimal Dark Matter

Marco Cirelli<sup>a</sup>, Alessandro Strumia<sup>b</sup>, Matteo Tamburini<sup>c</sup>

<sup>a</sup> *Service de Physique Théorique, CEA-Saclay, France and INFN, Italy*

<sup>b</sup> *Dipartimento di Fisica dell'Università di Pisa and INFN, Italia*

<sup>c</sup> *Dipartimento di Fisica dell'Università di Pisa*

## Abstract

We consider DM that only couples to SM gauge bosons and fills one gauge multiplet, e.g. a fermion 5-plet (which is automatically stable), or a wino-like 3-plet. We revisit the computation of the cosmological relic abundance including non-perturbative corrections. The predicted mass of e.g. the 5-plet increases from 4.4 TeV to 10 TeV, and indirect detection rates are enhanced by 2 orders of magnitude. Next, we show that due to the quasi-degeneracy among neutral and charged components of the DM multiplet, a significant fraction of DM with energy  $E \gtrsim 10^{17}$  eV (possibly present among ultra-high energy cosmic rays) can cross the Earth exiting in the charged state and may in principle be detected in neutrino telescopes.

## Contents

<b>1</b>	<b>Introduction</b>	<b>2</b>
<b>2</b>	<b>Non perturbative Sommerfeld corrections</b>	<b>2</b>
2.1	Computing Sommerfeld corrections . . . . .	5
<b>3</b>	<b>Cosmological abundances</b>	<b>7</b>
<b>4</b>	<b>Indirect detection of Minimal Dark Matter</b>	<b>13</b>
<b>5</b>	<b>Minimal Dark Matter at Ultra High Energies</b>	<b>15</b>
5.1	Propagation of UHE Minimal Dark Matter . . . . .	15
5.2	Production of UHE Minimal Dark Matter . . . . .	18
5.3	Detection of UHE DM <sup>±</sup> . . . . .	20
<b>6</b>	<b>Conclusions</b>	<b>20</b>
<b>A</b>	<b>Annihilation cross sections</b>	<b>22</b>

# 1 Introduction

Observations and experiments tell that:

- i) Dark Matter (DM) exists [1], with abundance  $\Omega_{\text{DM}}h^2 = 0.110 \pm 0.005$  [2];
  - ii) DM is cosmologically stable; it has no electric charge [3], no strong interactions [4] and the DM coupling to the  $Z$  boson is smaller than  $\sim 10^{-3}g_2$  [5].
- i) suggests that DM might be a weak-scale particle: indeed  $\Omega_{\text{DM}} \sim 1$  is the typical freeze-out abundance of a typical particle with weak-scale mass  $M$  and coupling  $g$ :  $M/g \sim \sqrt{T_0 M_{\text{Pl}}} \sim \text{TeV}$ . ii) can be satisfied in appropriate models, although these properties are not typical weak scale particles.

We here want to study Minimal DM (MDM) models: we add to the Standard Model (SM) one new multiplet, that only has gauge interactions and a  $\text{SU}(2)_L$ -invariant mass term  $M$ . In this context, ii) singles out scalars or fermions with zero hypercharge that fill a  $\text{SU}(2)_L$  representation with odd dimension:  $n = 3, 5, \dots$  [6]. The neutral  $\text{DM}^0$  component is then lighter than the charged  $\text{DM}^\pm$  components, by only 166 MeV.  $\text{DM}^0$  interacts with ordinary matter via one-loop exchange of  $W^\pm$ : future direct DM searches will hopefully reach the sensitivity needed to detect it.

The fermion 5-plet is particularly interesting: all interactions other than the gauge interactions are incompatible with gauge and Lorentz symmetries [6], so that it is automatically stable thanks to an accidental symmetry, like the proton in the SM. Other candidates that we will consider lack this feature (i.e. some extra symmetry is responsible for their stability) but are also interesting. The fermion 3-plet is well known from supersymmetry with matter-parity, as ‘pure wino’ DM; the fermion doublet case as ‘pure higgsino’ DM. We will also study scalar MDM candidates. In general, this scenario has one free parameter, the DM mass  $M$ , already fixed by  $\Omega_{\text{DM}}$ , such that all DM signals are univocally predicted. We here address the following issues.

First, we complete the computation of the cosmological abundance performed in [6] taking into account  $p$ -wave annihilations and renormalization of the gauge couplings up to the DM scale, and, more importantly, we include non-perturbative Sommerfeld corrections: the DM wave-functions get distorted by Coulomb-like forces mediated by SM vectors. Their relevance was pointed out in [7], in the case of gluino and wino as lightest supersymmetric particle. In section 2 we discuss the basic physics of non-perturbative Sommerfeld corrections, and in section 3 we show our results for the cosmological DM abundance.

Next, in section 4 we compute the  $\text{DM}^0\text{DM}^0$  annihilation rates relevant for indirect MDM signals, including the sizable enhancement due to Sommerfeld corrections.

Finally, in section 5 we study the possibility that the ultra-high-energy cosmic rays (UHE CR) contain some DM particle (although this looks difficult within the standard CR acceleration mechanism), showing that MDM candidates can cross the earth arriving to the detector in the charged state. We discuss how it could manifest in detectors such as neutrino telescopes.

Section 6 presents our conclusions.

## 2 Non perturbative Sommerfeld corrections

If the DM mass is  $M \approx M_Z$  and if the DM coupling is  $g \approx g_2$ , DM DM annihilations into SM vectors have a too large cross section, and consequently give a too low freeze-out DM

abundance. Since  $\Omega_{\text{DM}} \propto M$  for  $M > M_Z$ , the observed DM abundance is obtained for a value of  $M$  sufficiently larger than  $M_Z$ .<sup>1</sup> Since this value turns out to be in the TeV or multi-TeV range, we can ignore SM particle masses when computing the annihilation rates. Using SU(2) algebra, ref. [6] obtained a single expression for the cosmological abundance of any MDM candidate, taking into account all (co-)annihilations in  $s$ -wave approximation. We here add  $p$ -wave annihilations and renormalization of the gauge couplings up to the DM mass  $M$ : each one of these effects gives a  $\mathcal{O}(5\%)$  correction to  $\Omega_{\text{DM}}$ . Precise formulæ are given in appendix A.

Furthermore, we take into account non-perturbative electroweak Sommerfeld corrections. Their relevance was pointed out in [7] and might look surprising, so we start with a general semi-quantitative discussion before proceeding with the detailed computations. Scatterings among charged particles due to point-like interactions are distorted by the Coulomb force, when the kinetic energy is low enough that the electrostatic potential energy is relevant. This leads e.g. to significant enhancements of the  $\mu^- \mu^+$  annihilation cross section (attractive force) or to significant suppressions of various nuclear processes (repulsive force). These effects can be computed with a formalism developed by Sommerfeld [9]. In the language of Feynman graphs, these effects are described by multi-loop photon ladder diagrams. Perturbative computations would include only the first few diagrams: the Sommerfeld enhancement is non-perturbative because a resummation of all ladder diagrams is needed.<sup>2</sup> The generalization of the Sommerfeld formalism to the case of DM DM annihilations, that involves non abelian massive vectors, was presented in [10].

Let us first discuss Sommerfeld corrections due to one abelian vector with mass  $M_V$  and gauge coupling  $\alpha$ : this case already contains the relevant physics and can be analyzed in a simpler way. Cross sections at low energies are dominated by  $s$ -wave scattering, with  $p$ -wave giving corrections of relative order  $T/M$ . Since the DM DM annihilation is local (i.e. it occurs when the distance between the two DM particles is  $r \simeq 0$ ), the non perturbative correction is given by  $R = |\psi(\infty)/\psi(0)|^2$ , where  $\psi(r)$  is the (reduced)  $s$ -wave-function for the two-body DM state with energy  $K$ , that in the non-relativistic limit satisfies the Schrödinger equation

$$-\frac{1}{M} \frac{d^2 \psi}{dr^2} + V \cdot \psi = K \psi \quad V = \pm \frac{\alpha}{r} e^{-M_V r} \quad (1)$$

with outgoing boundary condition  $\psi'(\infty)/\psi(\infty) \simeq iM\beta$ . Here  $K = M\beta^2$  is the kinetic energy of the two DM particles in the center-of-mass frame, where each DM particle has velocity  $\beta$ . The  $-$  sign corresponds to an attractive potential and the  $+$  sign to a repulsive potential. We define  $\epsilon \equiv M_V/M$ , the adimensional ratio between the vector mass and the DM mass.

Eq. (1) is the prototype of the equations that describe corrections to  $\text{DM}^0 \text{DM}^0$  annihilations mediated by a  $Z$  boson, or  $\text{DM}^+ \text{DM}^-$  or  $\text{DM}^+ \text{DM}^+$  co-annihilations mediated by a  $\gamma$  or  $W$  or  $Z$ , or corrections mediated by a gluon (in models where coannihilations with and between colored particles are relevant). In the three cases, the coupling  $\alpha$  that appears in eq. (1) would be  $\alpha_2$ ,  $\alpha_{\text{em}}$  and  $\alpha_s$  respectively. In the non abelian case, eq. (1) becomes a matrix equation and

---

<sup>1</sup> Another solution exists for  $M$  sufficiently lower than  $M_Z$ , such that annihilation into vectors are kinematically suppressed. In the minimal scenario that we consider, this solution is excluded by LEP2 and other collider data, but in general it is still allowed in some part of the parameter range of non-minimal scenarios [8].

A DM mass  $M \approx M_Z$  can of course also be obtained by reducing  $g$ , i.e. by assuming that DM is any SU(2)<sub>L</sub> multiplet appropriately mixed with a singlet.

<sup>2</sup> Sometimes in the literature ‘non-perturbative’ is used with a different meaning: to denote effects that vanish in the perturbative limit because suppressed e.g. by  $e^{-1/\alpha}$  factors.

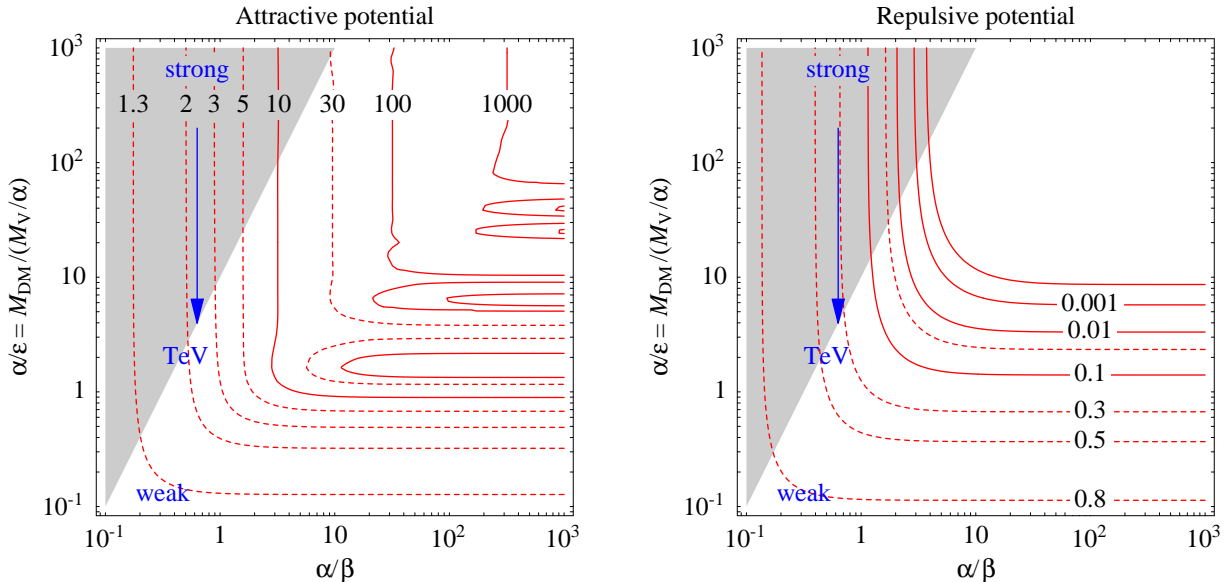


Figure 1: Iso-contours of the non-perturbative Sommerfeld correction to the DM DM annihilation. Here  $\alpha$  is the coupling constant,  $\beta$  is the DM velocity,  $\epsilon$  is the ratio between the vector mass and the DM mass. The labels indicate where some classes of DM candidates lie in this plane: ‘weak’ indicates weak-scale DM particles, ‘TeV’ indicates DM with multi-TeV mass, and ‘strong’ indicates strongly-interacting particles that in some models give dominant co-annihilations. Within the shaded region thermal masses dominate over masses, effectively shifting the value of  $\alpha/\epsilon$  as indicated by the arrow.

$V$  is the sum of the various contributions mediated by all SM vectors. Higgs exchange can also be relevant, in models where DM sizably couples to the Higgs.

For  $\epsilon = 0$  (massless vector) the Schrödinger equation has the same form as the one that describes e.g. the hydrogen atom, and it can be analytically solved: the Sommerfeld factor  $R$  that multiplies the perturbative cross section is

$$R = \frac{-\pi x}{1 - e^{-\pi x}} \quad x = \pm \frac{\alpha}{\beta} \quad (\text{for } M_V = 0) \quad (2)$$

This shows that  $R$  sizably differs from 1 at  $\beta \lesssim \pi\alpha$ . DM DM annihilations into SM particles freeze-out when the temperature  $T$  cools down below  $T/M \sim 1/\ln(M_{\text{Pl}}/M) \sim 1/26$ . This happens to be numerically comparable to the SM gauge couplings, i.e.  $\alpha_2 \approx 1/30$ . Consequently DM freeze-out occurs when  $\beta \sim 0.2$  i.e.  $\pi x \sim 1$ : the Sommerfeld correction is significant,  $R \sim \mathcal{O}(1)$ .

Of course we must take into account that the relevant  $W, Z$  vectors are massive: since  $R$  must now be computed numerically, it is convenient to first identify on which parameters  $R$  depends. We notice that  $R$  only depends on the two ratios  $\alpha/\beta$  and  $\alpha/\epsilon$ , so that  $R$  can be plotted on a plane. This can be proved noticing that  $R$  is adimensional and that physics is invariant under  $r \rightarrow \lambda r$ ,  $M \rightarrow M/\lambda$ ,  $M_V \rightarrow M_V/\lambda$ . Fig. 1 shows iso-contours of  $R$  as function of  $\alpha/\beta$  and  $\alpha/\epsilon$ . We can distinguish various regions:

- a) Non-perturbative effects are negligible (i.e.  $|R - 1| \ll 1$ ) if  $\pi\alpha \ll \beta$  and/or if  $\alpha \ll \epsilon$ . We have seen that  $\pi\alpha \sim \beta$ , so non-perturbative effects are relevant when  $M \gtrsim M_V/\alpha$ , where  $M_V$  are the SM vector masses and  $\alpha$  are their gauge couplings [10].
- b) If  $\beta \lesssim \epsilon \lesssim \alpha$  ('lower triangle region')  $\beta$  is so low that its value is no longer relevant:  $R$  depends only on  $\alpha/\epsilon$  showing, in the attractive case, a series of resonances. Indeed, by increasing  $\alpha/\epsilon$  the potential develops more and more bound states: resonant enhancement happens when a bound state first appears with energy  $E_B$  just below zero: in this case, at low energy  $R$  depends on  $K$  as dictated by a Breit-Wigner factor  $1/(K - E_B)$ .
- c) If  $\epsilon \lesssim \beta \lesssim \alpha$  ('upper triangle region') non-perturbative effects depend almost only on  $\alpha/\beta$ : vector masses have a minor effect and  $R$  reduces to eq. (2). Its value does not depend on whether a loosely bound resonance is present or not.

When DM DM bound states are relevant, the Sommerfeld correction might not encode the full dynamics: one should compute the density and life-time of DM DM bound states.

We include one more effect, not discussed in [7]. At finite temperature  $T$ , the  $\gamma, Z, W$  masses and the mass splitting  $\Delta M$  between the components of the DM multiplet are different than at zero temperature. First, because these masses are proportional to the SU(2)-breaking Higgs vev  $v$ , that depends on  $T$  and vanishes at  $T > T_c$  when SU(2) invariance gets restored by thermal effects, via a second-order phase transition. This effect can be roughly approximated as [11]

$$v(T) = v \operatorname{Re}(1 - T^2/T_c^2)^{1/2}. \quad (3)$$

The critical temperature  $T_c$  depends on the unknown Higgs mass ( $T_c \simeq m_H$  for  $m_H \gg v$ ): we here assume  $T_c = 200$  GeV.

Second, the squared masses of all SM vectors  $W, Z, \gamma, g$  get an extra contribution known as thermal mass. More precisely, even in the non abelian case, the Coulomb force gets screened by the thermal plasma: this can be described by a vector Debye mass, equal to [12]

$$m_{U(1)}^2 = \frac{11}{6} g_Y^2 T^2, \quad m_{SU(2)}^2 = \frac{11}{6} g_2^2 T^2, \quad m_{SU(3)}^2 = 2g_3^2 T^2 \quad (4)$$

in the SM at  $T \gg M_{W,Z}$ . We approximate vector masses by summing the squared masses generated from  $v(T)$  with the SU(2)-invariant Debye squared masses of eq. (4).

Let us now estimate the relevance of these thermal effects. For the  $W$  and  $Z$  bosons, thermal masses dominate at  $T \gtrsim v$ , and for the photon and the gluons thermal masses dominate always. At temperature  $T$  DM particles have a typical energy  $K \approx T$ , so that thermal masses act like a contribution to  $\epsilon$  of order  $\epsilon_T \sim \sqrt{4\pi\alpha}\beta^2$ . When this thermal effect is relevant, in fig. 1 one has to shift  $\alpha/\epsilon$  vertically down to the diagonal of the shaded triangle: we see that (depending on the precise value of  $\alpha/\beta$ ) this shift has a mild or negligible effect on  $R$ , since thermal effects are relevant when  $R$  does not have a significant dependence on  $\epsilon$ .

## 2.1 Computing Sommerfeld corrections

Following [7, 10], we now give a operative summary about how to compute Sommerfeld corrections to  $s$ -wave DM DM annihilation rates. The set of two-body  $DM_i DM_j$  states that mix among them is labeled as  $i, j = \{1, \dots, N\}$ . For example, when studying the wino triplet one

encounters the  $\{\text{DM}^-\text{DM}^+, \text{DM}^0\text{DM}^0\}$  system. The dynamics is encoded in the  $N \times N$  potential matrix  $V$  and in another  $N \times N$  matrix  $\Gamma$ , that describe the tree-level (co)-annihilation rates. The strategy is the same as in the abelian case of eq. (1), plus a careful book-keeping of indices. For each  $j$  one solves the following set of  $N$  coupled differential equations for  $\psi_i^{(j)}(r)$ :

$$-\frac{1}{M} \frac{\partial^2 \psi_i^{(j)}}{\partial r^2} + \sum_{i'=1}^N V_{ii'} \psi_{i'}^{(j)} = K \psi_i^{(j)} \quad (5)$$

with boundary conditions:

$$\psi_i^{(j)}(0) = \delta_{ij}, \quad \frac{\partial \psi_i^{(j)}(\infty)}{\partial r} = \sqrt{M(K - V(\infty)_{ii})} \psi_i^{(j)}(\infty) \quad (6)$$

chosen such that each wave has the same normalization at  $r = 0$ , where the annihilation occurs as described by the  $\Gamma$  matrices. The annihilation cross section  $\sigma_i$  with given initial state  $i$  at  $r = \infty$  is obtained by factorizing out the oscillating phase,  $A_{ij} \equiv \lim_{r \rightarrow \infty} \psi_i^{(j)}(r) / e^{i\Re \sqrt{M(K - V(\infty))}r}$ , and contracting with the annihilation matrix:

$$\sigma_i = c_i (A \cdot \Gamma \cdot A^\dagger)_{ii} \quad (7)$$

The factor  $c_i$  is given by  $c_i = 2$  if the initial state  $i$  has two equal DM particles (e.g. as in the  $\text{DM}^0\text{DM}^0$  state) and  $c_i = 1$  otherwise (e.g. as in the  $\text{DM}^-\text{DM}^+$  state). This formalism automatically takes into account that some states cannot exist as free particles at  $r \gg 1/M_W$ , when the kinetic energy  $K$  is below their mass.

We next need to compute the Coulomb-like potential matrices  $V$  and the tree-level annihilation matrices  $\Gamma$  for all DM components. They split into sub-systems with given values of the  $L$  (orbital angular momentum),  $S$  (total spin) and  $Q$  (total electric charge) quantum numbers. Recalling that we neglect SM particle masses and that we consider  $s$ -wave (i.e.  $L = 0$ ) tree-level annihilations into two SM particles, annihilations obey the following selection rules:

- 0) two-body DM DM states with spin  $S = 0$  can annihilate into two SM vectors, that can have electric charge  $Q = 0, \pm 1, \pm 2$ .
- 1) two-body DM DM states with spin  $S = 1$  can annihilate into two SM fermions and into two SM Higgses, that can have electric charge  $Q = 0, \pm 1$ .<sup>3</sup>

The initial DM DM state with  $S = 1$  of case 1) does not exist if DM is a scalar.<sup>4</sup>

We now give explicit expressions for the annihilation matrices  $\Gamma_{ii',jj'}$  and potential matrices  $V_{ii',jj'}$ . Their off-diagonal entries do not have an intuitive physical meaning, and are precisely

---

<sup>3</sup>Non-perturbative corrections are mostly relevant when  $\text{SU}(2)_L$  is unbroken: in this limit one could perform a simplified analysis by replacing the electric charge quantum number with the  $\text{SU}(2)_L$  isospin quantum number  $I$ . Then, the only DM DM states that can annihilate into SM particles are those with  $S = 0$  and  $I = 1$  and 5 (that annihilate into SM vectors;  $I = 1$  indicates the singlet) and the state with  $S = 1$  and  $I = 3$  (that annihilates into SM fermions and Higgses.).

<sup>4</sup> These selection rules also apply to  $\text{DM}^0 \text{DM}^0$  annihilations relevant for indirect astrophysical DM signals, and reproduce well known results. E.g. if  $\text{DM}^0$  is a Majorana fermion the spin-statistics relation forbids  $S = 1$ , so that annihilations into vectors are not possible. A non vanishing amplitude for  $\text{DM}^0 \text{DM}^0 \rightarrow f\bar{f}$ , proportional to  $m_f$ , is allowed when one takes into account the small mass  $m_f$  of the SM fermions  $f$ .

defined in terms of the imaginary part and of the real part of the two-body propagator  $ii' \rightarrow jj'$ , where the indices  $ii'$  denote the two DM component in the initial state, and  $jj'$  denote the two DM components in the final state.

For MDM scalars with  $Y = 0$  one has (all states have  $S = 0$ )

$$\Gamma_{ii',jj'} = \frac{N_{ii'}N_{jj'}}{8\pi n g_{\text{DM}} M^2} \sum_{A,B} \{T^A, T^B\}_{ii'} \{T^A, T^B\}_{jj'} \quad (8a)$$

$$V_{ii',jj'}(r) = (M_i + M_j - M) \delta_{ii'} \delta_{jj'} + N_{ii'} N_{jj'} \sum_{AB} K_{AB} (T_{ij}^A T_{i'j'}^B + T_{ij'}^A T_{ij}^B) \frac{e^{-m_A r}}{r} \quad (8b)$$

where  $N_{ij} = 1$  if  $i \neq j$  and  $1/\sqrt{2}$  if  $i = j$ . The indices  $A, B$  run over the SM vectors  $\{\gamma, Z, W^+, W^-\}$  with generators  $T^A$  in the DM representation. The gauge couplings are included in the generators, such that the gauge-covariant derivative is  $D_\mu = \partial_\mu + iA_\mu^A T^A$ . We emphasize that the (off-diagonal) entries of  $T^\pm$  are defined up to an arbitrary phase normalization for each component of the multiplet: one needs to choose any convention such that the SU(2)-invariant DM mass term has the same sign for all DM components. The matrices  $K_{AB}$  and  $C_{AB}$  respectively describe SM vector propagation and the gauge content of all other SM particles, and are given by:

$$K_{AB} = \begin{pmatrix} 1 & 0 & 0 & 0 \\ 0 & 1 & 0 & 0 \\ 0 & 0 & 0 & 1 \\ 0 & 0 & 1 & 0 \end{pmatrix}, \quad C_{AB} = \frac{25g_2^2}{4} \begin{pmatrix} s^2 & sc & 0 & 0 \\ sc & c & 0 & 0 \\ 0 & 0 & 0 & 1 \\ 0 & 0 & 1 & 0 \end{pmatrix} + \frac{41}{4} g_Y^2 \begin{pmatrix} c^2 & -sc & 0 & 0 \\ -sc & s^2 & 0 & 0 \\ 0 & 0 & 0 & 0 \\ 0 & 0 & 0 & 0 \end{pmatrix}.$$

For MDM fermions with  $Y = 0$  one has

$$\Gamma_{ii',jj'}^{S=0} = \frac{N_{ii'}N_{jj'}}{16\pi n g_{\text{DM}} M^2} \sum_{A,B} \{T^A, T^B\}_{ii'} \{T^A, T^B\}_{jj'} \quad (9a)$$

$$\Gamma_{ii',jj'}^{S=1} = \frac{N_{ii'}N_{jj'}}{8\pi n g_{\text{DM}} M^2} \sum_{A,B} T_{ii'}^A T_{jj'}^B C_{AB} \quad (9b)$$

$\Gamma^{S=1}$  is already summed over the 3 spin components. The potentials  $V$  remain the same as in the scalar case of eq. (8b), up to an extra  $-$  sign that must be taken into account when computing elements of  $V$  mediated by the  $W$ , such as  $V_{0-,0-} = -V_{0-,0}$ , because an extra  $-$  sign appears in the definition of two body fermion states:  $|\text{DM}^0 \text{DM}^- \rangle = -|\text{DM}^- \text{DM}^0 \rangle$ . Furthermore, Fermi statistics forbids the existence of some states, such as  $|\text{DM}^0 \text{DM}^0 \rangle$  with  $S = 1$ .

Similar formulæ apply to MDM candidates with  $Y \neq 0$ , after taking into account that  $\text{DM}^0$  now becomes a complex particle (its normalization factor changes from  $N_{00} = 1/2$  to  $N_{0\bar{0}} = 1$ ) and that one is only interested in DM  $\bar{\text{DM}}$  annihilations and two body states. Summing  $\Gamma_{ii',ii'}$  over all components one reproduces the total co-annihilation rates of [6], here reported and extended in appendix A. Explicit expressions for  $V$  and  $\Gamma$  are given in the next sections.

### 3 Cosmological abundances

To include non-perturbative corrections a dedicated lengthy analysis is needed for each MDM candidate.

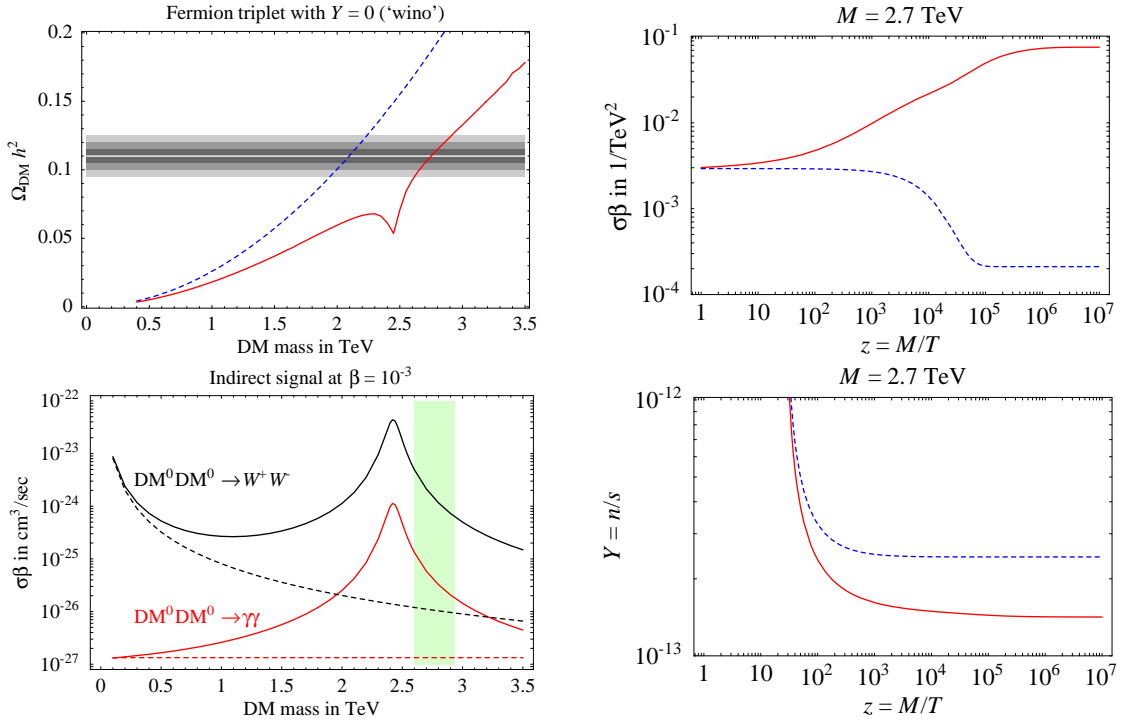


Figure 2: **The fermion triplet with zero hypercharge ('wino')**. Fig. 2a (upper left): our result for its cosmological freeze-out DM abundance as function of the DM mass. Fig. 2c (upper right) show an example (for the indicated mass  $M$ ) of the temperature dependence of the DM DM annihilation cross section, and fig. 2d (lower right) shows the resulting cosmological evolution of the DM abundance. Fig. 2b (lower left) shows our result for  $\text{DM}^0\text{DM}^0$  annihilation cross section relevant for indirect DM detection, as discussed in section 4. In each case, the continuous line is our full result, while the dashed line is the result obtained without including non-perturbative effects.

*The fermion triplet with  $Y = 0$  ('wino').*

It is not automatically stable: one needs to impose a suitable symmetry. Since  $Y = 0$  the lightest component of this multiplet is neutral under the  $\gamma$  and under the  $Z$ , and therefore it satisfies bounds from direct DM searches [13, 6]. This multiplet appears in supersymmetric models as  $\text{SU}(2)_L$  gauginos, and behaves as MDM in limiting cases where it is much lighter than other sparticles.

We include  $p$ -wave DM DM annihilations, but we only include non perturbative corrections to  $s$ -wave annihilations, that are splitted into four sectors with  $L = 0$ , total charge  $Q = \{0, 1\}$  and total spin  $S = \{0, 1\}$ . All sectors involve one component, except the sector with  $Q = 0$  and  $S = 0$ , that involves two components  $\{\text{DM}^-\text{DM}^+, \text{DM}^0\text{DM}^0\}$ . In this case and in the following we indicate the basis we employ by writing the charges of the DM components around the  $\Gamma$  and  $V$  matrices, and by indicating  $Q$  and  $S$  as pedices and apices on  $\Gamma$  and  $V$ . Using eq. (9), for the fermion triplet we get:

$$\Gamma_{Q=0}^{S=0} = \frac{\pi\alpha_2^2}{9M^2} \begin{matrix} + & 0 \\ \begin{pmatrix} 3 & \sqrt{2} \\ \sqrt{2} & 2 \end{pmatrix} \end{matrix}, \quad V_{Q=0}^{S=0} = \begin{matrix} + & 0 \\ \begin{pmatrix} 2\Delta - A & -\sqrt{2}B \\ -\sqrt{2}B & 0 \end{pmatrix} \end{matrix}, \quad (10)$$



$$\Gamma_{Q=0}^{S=1} = \frac{25\pi\alpha_2^2}{36M^2} \quad V_{Q=0}^{S=1} = 2\Delta - A \quad (11)$$

$$\Gamma_{Q=1}^{S=0} = \frac{\pi\alpha_2^2}{9M^2}, \quad \Gamma_{Q=1}^{S=1} = \frac{25\pi\alpha_2^2}{36M^2}, \quad V_{Q=1}^{S=0,1} = \Delta - B \quad (12)$$

$$\Gamma_{Q=2}^{S=0} = \frac{\pi\alpha_2^2}{9M^2}, \quad V_{Q=2}^{S=0} = 2\Delta + A. \quad (13)$$

where  $\Delta = 166 \text{ MeV}$ ,  $A = \alpha_{\text{em}}/r + \alpha_2 c_{\text{W}}^2 e^{-Mzr}/r$  and  $B = \alpha_2 e^{-Mwr}/r$ . These results are equivalent to those of [7].

We numerically solve the Schrödinger equations use the finite-temperature values for  $\Delta$  and vector masses (e.g.  $\Delta$  vanishes when  $\text{SU}(2)_L$ -invariance is restored, etc.). Fig. 2a shows our result for its freeze-out cosmological abundance: as previously noticed in [7] non-perturbative corrections are relevant, and significantly increase the multi-TeV value of  $M$  that reproduces the measured cosmological abundance. In the supersymmetric case, a multi-TeV wino lightest supersymmetric particle implies a fine-tuning in the Higgs mass above the  $10^3$  level, so that this scenario seems not motivated by the Higgs mass hierarchy problem.

A bound state first appears for  $M > M_* \approx 2.5 \text{ TeV}$ , in the DM DM system with total charge  $Q = 0$  and total spin  $S = 0$ . Fig. 2c and d show more details of the computation for  $M = 2.7 \text{ TeV}$ . Since  $M$  is just above  $M_*$ , the bound state is loosely bound,  $E_B \approx -67 \text{ MeV}$ , and gives rise to a significant non-perturbative enhancement  $R$  of the annihilation cross section, apparent in fig. 2c as a dip at  $M = M_*$ . The result is reliable, because temperatures  $T \lesssim |E_B|$  (at which a dedicated treatment of bound states would be necessary) do not significantly affect the final cosmological abundance, as indicated by fig. 2d and by the fact that the dip is not the main effect.

*The scalar triplet with  $Y = 0$ .*

This MDM candidate is not automatically stable: one needs to impose a suitable symmetry. Having  $Y = 0$ , this candidate is compatible with bounds from direct DM searches. Any  $\text{SU}(2)_L$  multiplet of scalars can have a quartic interaction with the Higgs,  $-\lambda_H (\mathcal{X}^\dagger T^a \mathcal{X})(H^\dagger \tau^a H)$ , that generates a tree-level mass splitting within the multiplet. Since this mass splitting is suppressed by the DM mass  $M$  [6] it is not unbelievable that scalars behave as MDM because  $\lambda_H$  is small enough,  $\lambda_H \ll 0.05$ , that the  $\Delta = 166 \text{ MeV}$  mass splitting induced by gauge couplings is dominant. This is particularly plausible in the case of scalars with  $Y = 0$ , because  $\lambda_H$  is not generated by one-loop RGE corrections. Indeed RGE corrections that induce a  $\lambda_H$  proportional to  $g_2^2$  happen to vanish, because the Higgs  $H$  is a doublet, and the doublet representation of  $\text{SU}(2)_L$  has vanishing symmetric tensor:  $\text{Tr } T_H^a \{T_H^b, T_H^c\} = 0$ .

To include non-perturbative corrections to DM DM annihilations we split them into three sectors, with  $L = 0$ ,  $S = 0$  and total charge  $Q = \{0, 1, 2\}$ . The  $V$  and  $\Gamma$  matrices are

$$\Gamma_{Q=0}^{S=0} = \frac{2\pi\alpha_2^2}{9M^2} \begin{matrix} + & 0 \\ \left( \begin{array}{cc} 3 & \sqrt{2} \\ \sqrt{2} & 2 \end{array} \right) \end{matrix}, \quad V_{Q=0}^{S=0} = \begin{matrix} + & 0 \\ - \left( \begin{array}{cc} 2\Delta - A & -\sqrt{2}B \\ -\sqrt{2}B & 0 \end{array} \right) \end{matrix}, \quad (14)$$

$$\Gamma_{Q=1}^{S=0} = \frac{2\pi\alpha_2^2}{9M^2}, \quad V_{Q=1}^{S=0} = \Delta + B, \quad \Gamma_{Q=2}^{S=0} = \frac{2\pi\alpha_2^2}{9M^2}, \quad V_{Q=2}^{S=0} = 2\Delta + A. \quad (15)$$

Fig. 3a shows our result for its freeze-out cosmological abundance: non-perturbative corrections are again important. Fig. 3c and d show details of the computation for  $M = 2.5 \text{ TeV}$ , a

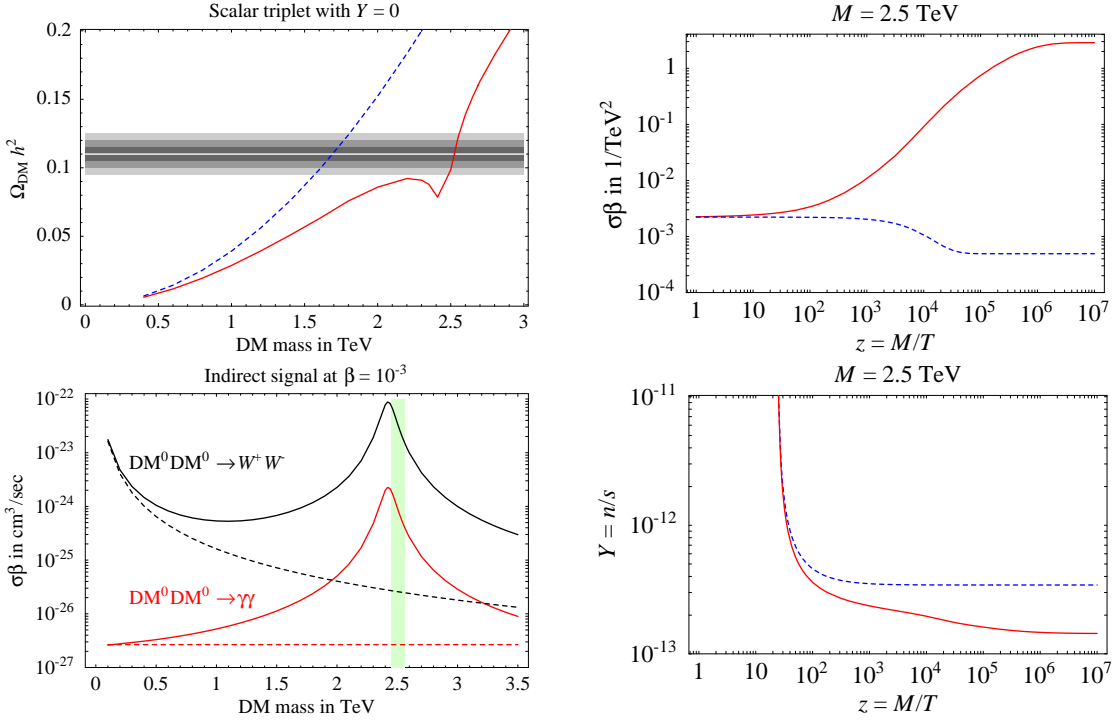


Figure 3: *The scalar triplet with zero hypercharge. Plots have the same meaning as in fig. 2.*

mass close to the critical mass  $M_* \approx 2.5$  TeV at which a bound state appears in the DM DM system with total charge  $Q = 0$ .

We here do not study scalar and fermion triplets with  $|Y| = 1$ ; the neutral component has  $T_3 = Y \neq 0$  and consequently couples to the  $Z$ , giving a too large direct detection rate. A non-minimal mixing with a singlet is needed to avoid this problem. One expects significant non-perturbative corrections, similarly to the  $Y = 0$  case, as  $SU(2)_L$  gauge interactions are more significant than  $U(1)_Y$  the extra gauge interaction.

*The fermion quintuplet with  $Y = 0$ .*

This is the smallest multiplet whose lightest component is neutral under the  $\gamma$  and under the  $Z$  and is automatically stable on the cosmological timescale. Indeed gauge couplings are the only renormalizable interactions (compatible with gauge and Lorentz invariance) that this multiplet can have with other SM particles. Its phenomenology is univocally dictated by a single parameter: its Majorana mass  $M$ .

To include non-perturbative corrections to DM DM annihilations we split these scatterings into four  $L = 0$  sectors, with total spin  $S = \{0, 1\}$  and total charge  $Q = \{0, 1, 2\}$ . The  $Q = 0$  and  $S = 0$  system is composed by 3 states:

$$V_{Q=0}^{S=0} = \begin{matrix} & \begin{matrix} -- & - & 0 \end{matrix} \\ \begin{matrix} ++ \\ + \\ 0 \end{matrix} & \begin{pmatrix} 8\Delta - 4A & -2B & 0 \\ -2B & 2\Delta - A & -3\sqrt{2}B \\ 0 & 0 & -3\sqrt{2}B \end{pmatrix}, \end{matrix} \quad \Gamma_{Q=0}^{S=0} = \frac{3\pi\alpha_2^2}{25M^2} \begin{matrix} & \begin{matrix} ++ & + & 0 \end{matrix} \\ \begin{matrix} -- \\ - \\ 0 \end{matrix} & \begin{pmatrix} 12 & 6 & 2\sqrt{2} \\ 6 & 9 & 5\sqrt{2} \\ 2\sqrt{2} & 5\sqrt{2} & 6 \end{pmatrix}, \end{matrix} \quad (16)$$

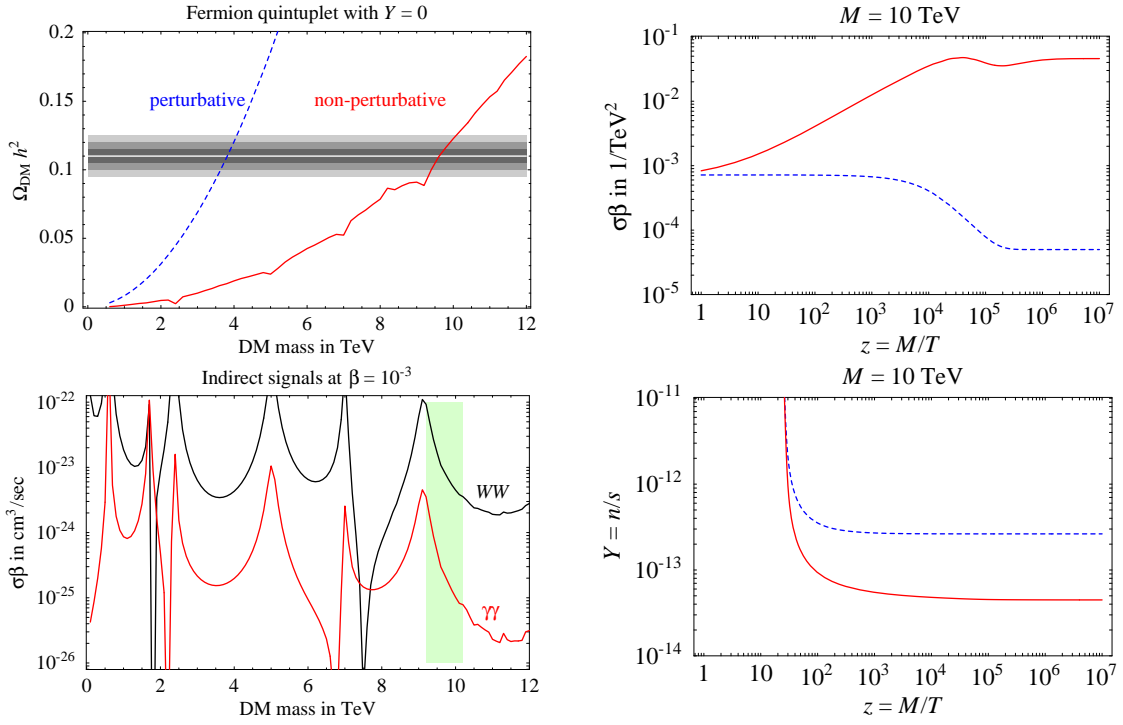


Figure 4: *The fermion quintuplet with zero hypercharge. Plots have the same meaning as in fig. 2.*

Due to Fermi statistics, the  $Q = 0, S = 1$  system has no  $DM^0DM^0$  state:

$$V_{Q=0}^{S=1} = \begin{array}{cc} & \begin{array}{cc} - & - \\ - & - \end{array} \\ \begin{array}{c} ++ \\ + \end{array} & \begin{pmatrix} 8\Delta - 4A & -2B \\ -2B & 2\Delta - A \end{pmatrix}, \quad \Gamma_{Q=0}^{S=1} = \frac{\pi\alpha_2^2}{4M^2} \begin{array}{cc} \begin{array}{cc} + & + \\ - & - \end{array} \\ \begin{array}{c} 4 \\ 2 \end{array} & \begin{array}{c} 2 \\ 1 \end{array} \end{array}, \quad (17)$$

The systems with  $Q = 1$  and  $S = \{0, 1\}$  have two states each:

$$V_{Q=1}^{S=0,1} = \begin{array}{cc} & \begin{array}{cc} + & + \\ - & + \end{array} \\ \begin{array}{c} - \\ 0 \end{array} & \begin{pmatrix} 5\Delta - 2A & -\sqrt{6}B \\ -\sqrt{6}B & \Delta - 3B \end{pmatrix}, \quad (18)$$

$$\Gamma_{Q=1}^{S=0} = \frac{3\pi\alpha_2^2}{25M^2} \begin{array}{cc} \begin{array}{cc} + & + \\ 0 & 0 \end{array} \\ \begin{array}{c} 6 \\ \sqrt{6} \end{array} & \begin{array}{c} \sqrt{6} \\ 1 \end{array} \end{array}, \quad \Gamma_{Q=1}^{S=1} = \frac{\pi\alpha_2^2}{4M^2} \begin{array}{cc} \begin{array}{cc} + & + \\ 0 & 0 \end{array} \\ \begin{array}{c} 2 \\ \sqrt{6} \end{array} & \begin{array}{c} \sqrt{6} \\ 3 \end{array} \end{array}. \quad (19)$$

Finally, in the systems with  $Q = 2$  the tree-level annihilation rate  $\Gamma$  is non vanishing only for  $S = 0$ :

$$V_{Q=2}^{S=0} = \begin{array}{cc} & \begin{array}{cc} + & + \\ - & + \end{array} \\ \begin{array}{c} 0 \\ + \end{array} & \begin{pmatrix} 4\Delta & -2\sqrt{3}B \\ -2\sqrt{3}B & 2\Delta + A \end{pmatrix}, \quad \Gamma_{Q=2}^{S=0} = \frac{3\pi\alpha_2^2}{25M^2} \begin{array}{cc} \begin{array}{cc} + & + \\ 0 & 0 \end{array} \\ \begin{array}{c} 4 \\ -\sqrt{12} \end{array} & \begin{array}{c} \sqrt{12} \\ 3 \end{array} \end{array}. \quad (20)$$

Fig. 4a shows our result for its freeze-out cosmological abundance: the value of  $M$  that reproduces the measured DM abundance was  $M \approx 4.4 \text{ TeV}$ . It slightly decreases down to

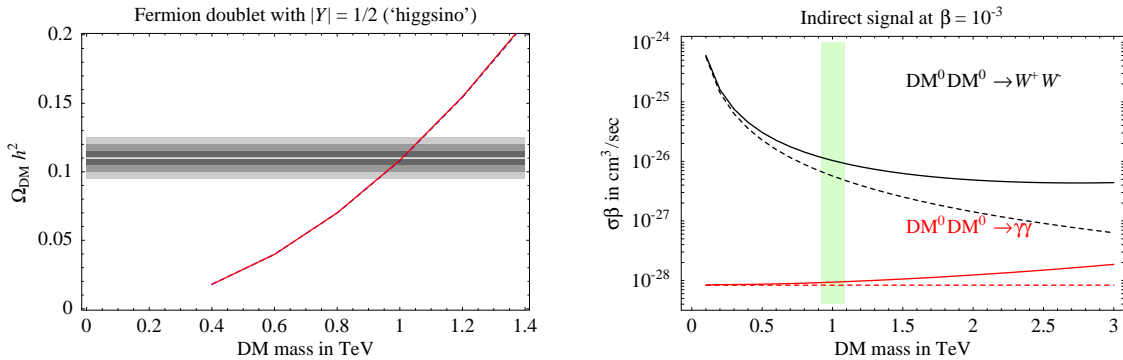


Figure 5: *Cosmological freeze-out abundance of the fermion doublet with  $Y = 1/2$  ('Higgsino'). Plots have the same meaning as in fig. 2, except that since non-perturbative corrections negligibly affect the cosmological abundance we do not show details of the computations.*

$M \approx 3.8 \text{ TeV}$  after including  $p$ -wave and RGE corrections (perturbative result in fig. 4a), and increases up to almost  $M \approx 10 \text{ TeV}$  after including the non-perturbative Sommerfeld corrections. Fig. 4d shows that Sommerfeld corrections are mostly relevant when  $T \gg \Delta M$ , such that bound states are not expected to play a relevant rôle.

*The scalar quintuplet with  $Y = 0$ .*

As in the scalar triplet case, is plausible to assume that the quartic coupling with the Higgs is negligibly small, because it is not generated by RGE effects. The  $V$  and  $\Gamma$  matrices are related to those relevant for the fermion 5-plet as described in section 2.1. Non-perturbative corrections increase the value of the mass  $M$  that reproduces the cosmological abundance from  $M \approx 5.0 \text{ TeV}$  [6] to  $M \approx 9.4 \text{ TeV}$ .

*The scalar septuplet with  $Y = 0$ .*

This is the smallest scalar multiplet that is automatically stable (its cubic scalar coupling identically vanishes) and contains a MDM candidate compatible with all bounds. Again, it is plausible to assume that the quartic coupling with the Higgs is negligibly small. Although we do not show dedicated plots nor the  $V$  and  $\Gamma$  matrices, we computed non-perturbative corrections finding that they increase the value of the mass  $M$  that reproduces the cosmological abundance from  $M \approx 8.5 \text{ TeV}$  [6] to about  $M \approx 25 \text{ TeV}$ .

*The fermion doublet with  $Y = 1/2$  ('Higgsino').*

It is not automatically stable, and, having  $Y \neq 0$ , is excluded by direct DM searches. Nevertheless, we consider it because  $n = 2$  is the smallest multiplet, and because it is present in supersymmetric models. The first problem can be solved by imposing a suitable symmetry, and incompatibility with direct detection experiments can be avoided by assuming a mass mixing with a neutral Majorana singlet (automatically present in supersymmetric models and known as 'bino'). We assume that this mass mixing is small enough not to affect the observables we compute. An almost-pure Higgsino LSP is realized in corners of the MSSM parameter space: it behaves as Minimal Dark Matter in the sense that its properties are not dictated by

supersymmetry but only by gauge invariance. In this limit, the  $\mu$ -term is the only relevant supersymmetric parameter, and coincides with our DM mass parameter  $M$ .

To include non-perturbative corrections to DM  $\overline{\text{DM}}$  annihilations we split these scatterings into four  $L = 0$  sectors, with total charge  $Q = \{0, 1\}$  and total spin  $S = \{0, 1\}$ . The  $\Gamma$  and  $V$  matrices that describe each sector are

$$\Gamma_{Q=0}^{S=0} = \frac{\pi\alpha_2^2}{64M^2} \begin{array}{c} + \\ \bar{0} \end{array} \begin{pmatrix} 3 + 2t^2 + t^4 & 3 - 2t^2 + t^4 \\ 3 - 2t^2 + t^4 & 3 + 2t^2 + t^4 \end{pmatrix}, \quad \Gamma_{Q=0}^{S=1} = \frac{\pi\alpha_2^2}{128M^2} \begin{array}{c} + \\ \bar{0} \end{array} \begin{pmatrix} 41t^4 + 25 & 41t^4 - 25 \\ 41t^4 - 25 & 41t^4 + 25 \end{pmatrix},$$

$$V_{Q=0}^{S=0,1} = \begin{array}{c} + \\ \bar{0} \end{array} \begin{pmatrix} -\alpha_{\text{em}}/r - (2c^2 - 1)^2 e^{-Mzr}/4rc^2 & -\alpha_2 e^{-Mwr}/2r \\ -\alpha_2 e^{-Mwr}/2r & -e^{-Mzr} \alpha_2/4rc^2 \end{pmatrix} \quad (21)$$

$$\Gamma_{Q=1}^{S=0} = \frac{\pi\alpha_2^2 t^2}{16M^2}, \quad \Gamma_{Q=1}^{S=1} = \frac{25\pi\alpha_2^2}{64M^2}, \quad V_{Q=1}^{S=0,1} = + \frac{\alpha_2 e^{-Mzr}}{r} \frac{2c^2 - 1}{4c^2} \quad (22)$$

where  $t = \tan\theta_W$ ,  $c = \cos\theta_W$  and  $\Delta = 341$  MeV is the mass splitting among charged and neutral components generated by loop effects. Fig. 5a shows our result for its cosmological abundance: in agreement with previous studies (e.g. [6]) we see that the observed DM abundance is reproduced for  $M = 1$  TeV. Non perturbative corrections are negligible. This also holds for the scalar doublet with  $|Y| = 1/2$ , so we do not study it.

The Higgs potential in the Minimal Supersymmetric Standard Model depends on the  $\mu$  parameter: a  $|\mu| = 1$  TeV gives a contribution to the squared  $Z$ -mass which is  $2\mu^2/M_Z^2 = 240$  times too large: therefore the Higgsino as Minimal Dark Matter can only be realized at the price of a sizable fine tuning.

## 4 Indirect detection of Minimal Dark Matter

We now study the usual ‘‘indirect DM signals’’, generated by  $\text{DM}^0 \text{DM}^0$  annihilations into SM particles. In the MDM case one only has tree-level annihilations into  $W^+W^-$ , while the most interesting final states,  $\gamma\gamma$  and  $\gamma Z$  (both detectable as  $\gamma$  with energy practically equal to  $E_\gamma = M$ ), arise at loop level. Assuming  $Y = 0$  the cross sections (averaged over DM polarizations) are, in the fermion DM case

$$\sigma(\text{DM}^0 \text{DM}^0 \rightarrow W^+W^-)\beta = (n^2 - 1)^2 \frac{\pi\alpha_2^2}{32M^2}, \quad \sigma(\text{DM}^0 \text{DM}^0 \rightarrow \gamma\gamma)\beta = (n^2 - 1)^2 \frac{\pi\alpha_{\text{em}}^2 \alpha_2^2}{16M_W^2}. \quad (23)$$

and 2 times higher in the scalar DM case. These cross-sections can be significantly affected by non-perturbative Sommerfeld corrections [10], because in our galaxy DM has a non-relativistic velocity  $\beta \approx 10^{-3}$ . The computation employs the same tools already described in the computation of DM DM annihilations relevant for cosmology. Non-perturbative effects can enhance the cross section by orders of magnitude for specific values of  $M$ : the values at which the potential develops a new bound state with  $Q, L, S = 0$ . In the triplet and quintuplet cases this enhancement is sizable, since the DM mass suggested by cosmology is close to one of such critical values. We show our results for the fermion triplet in fig. 2b, for the scalar triplet in fig. 3b, for the fermion quintuplet in fig. 4b, and for the fermion doublet in fig. 5b. The vertical

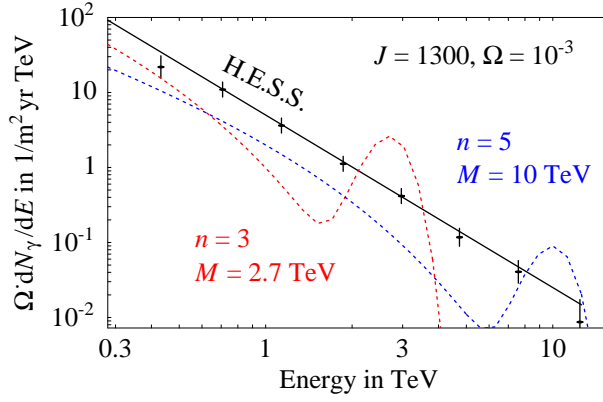


Figure 6: *Spectrum of  $\gamma$  from galactic  $\text{DM}^0\text{DM}^0$  annihilations, as seen by a detector with  $\Omega = 10^{-3}$ ,  $\sigma_E/E = 0.15$ . The total rate is computed assuming the NFW profile,  $J = 1300$ , and for fermion MDM with  $n = 3$  and  $M = 2.7$  TeV, and for  $n = 5$  and  $M = 10$  TeV. The continuous line is the H.E.S.S. result [14].*

bands are the  $3\sigma$  range of  $M$  suggested by cosmology. We have not plotted annihilation cross sections into  $\gamma Z$  and  $ZZ$  since all MDM candidates with  $Y = 0$  predict

$$\sigma_{\gamma Z} = 2\sigma_{\gamma\gamma}/\tan^2\theta_W = 6.5\sigma_{\gamma\gamma}, \quad \sigma_{ZZ} = \sigma_{\gamma\gamma}/\tan^4\theta_W = 10.8\sigma_{\gamma\gamma}. \quad (24)$$

These results allow to compute the energy spectra of annihilation products, such as photons, antiprotons, antideutrons and positrons. Note however that, precisely for the proximity to one of the critical values in mass, the cross sections depend strongly on the DM mass  $M$  and therefore the overall fluxes cannot be accurately predicted. Moreover, such total rates are affected by sizable astrophysical uncertainties. For example, the number of detected photons with energy  $E = M$  is [15]

$$N_\gamma(\text{at } E = M) \approx \frac{30}{\text{m}^2 \text{ yr sr}} J \Omega \left( \frac{\text{TeV}}{M} \right)^2 \frac{2\sigma_{\gamma\gamma}\beta + \sigma_{\gamma Z}\beta}{10^{-24} \text{ cm}^3/\text{s}}. \quad (25)$$

where  $\Omega$  is the angular acceptance of the detector and the quantity  $J$  ranges between a few and  $10^5$ , depending on the unknown DM density profile in our galaxy. Keeping these limitations in mind, fig. 6 shows the predicted energy spectrum of detected photons from MDM annihilations. We have assumed realistic detector parameters ( $\Omega = 10^{-3}$  and an energy resolution of 15%). The contribution from annihilations into  $W^+W^-$  is included using the spectral functions computed in [15, 10]. The total rate has an uncertainty of about two orders of magnitude and is here fixed assuming the indicated value of  $M$  and the Navarro-Frenk-White DM density profile,  $J = 1300$  [16, 1], which makes this signal at the level of the present sensitivity: Indeed the continuous line shows the spectrum of galactic  $\gamma$ ,  $dN_\gamma/dE \approx 5 \cdot 10^3 (\text{TeV}/E)^{2.3}/\text{m}^2 \text{ yr TeV sr}$ , as observed by H.E.S.S. [14] up to energies of about 10 TeV, where the number of events drops below one. Its spectral index suggests that the observed photons are generated by astrophysical mechanisms, rather than by DM DM annihilations. In view of the predicted value of  $\sigma_{\gamma\gamma}/\sigma_{WW}$ , the best MDM signal is the peak at  $E_\gamma = M$ . With the chosen parameters one gets  $N_\gamma = 0.3$  (2.6)/ $\text{m}^2 \cdot \text{yr}$  for the fermion 3-plet (5-plet).

## 5 Minimal Dark Matter at Ultra High Energies

In this section we discuss the possibility that Minimal Dark Matter might be detected via the tracks left by its charged partners in experiments mainly devoted to Cosmic Ray (CR) detection, such as Antares [17] or IceCUBE [18]. Indeed MDM behaves differently from other neutral particles:

- Neutrinos with energy  $E \lesssim 10^{15}$  eV can cross the whole Earth [19] and, impinging on the rock or ice below the detector, produce a charged partner (a muon, a tau) that cruises the instrumented volume.
- Neutral particles much heavier than neutrinos (e.g. the speculative neutralinos) interact rarely enough that they can cross the Earth even at Ultra High Energies (UHE),  $E \gg 10^{15}$  eV [20]. If they do interact before the end of their journey, they do produce a charged partner (e.g. the speculative chargino), that however usually decays almost immediately back to the neutral particle. For such reasons, it is generically difficult to detect them in this way.

MDM is both heavy and quasi-degenerate with a charged partner, leading to the following behavior. To be quantitative, we focus on MDM multiplets with  $Y = 0$ . They have a stable neutral DM particle,  $DM^0$ , and a charged  $DM^\pm$  component which is 166 MeV heavier. The latter dominantly decays via  $DM^\pm \rightarrow DM^0 \pi^\pm$  with a macroscopic life-time  $\tau = 44 \text{ cm}/(n^2 - 1)$  [6]. At Ultra High Energy Lorentz dilatation makes the  $DM^\pm$  life-time long enough that a sizable fraction of the travel is done as  $DM^\pm$ , leading to detectable charged tracks.<sup>5</sup>

This opens in principle an interesting and distinctive channel for the detection of DM. In order to assess its feasibility in practice, we need to study the system of MDM from production to detection. More precisely, first we study the issue of how a MDM system behaves when crossing the Earth at UHE, having assumed that the flux of UHE CR (observed up to  $E \sim 10^{20}$  GeV) does contain some DM particles. Mechanisms to produce such UHE DM are discussed later in section 5.2. We finally discuss detection signatures in section 5.3.

### 5.1 Propagation of UHE Minimal Dark Matter

Consider a flux of  $DM^0$  particles that is crossing the Earth at UHE. Via Charged Current (CC) interactions with nucleons of Earth's matter,  $DM^\pm$  particles are produced. Being charged particles traveling in a medium, these lose a part of their energy and eventually decay back to  $DM^0$  particles. This chain of production and decay is analogous to the process that tau neutrinos undergo in matter (“ $\nu_\tau$ -regeneration”). In the  $n = 5$  case  $DM^{\pm\pm}$  also play a role, but we will write explicit equations for the  $n = 3$  (wino-like) case. Such a system is described by a pair of coupled integro-differential equations for the evolution with the position  $\ell$  of fluxes  $n_0 = dN_0/dE$  and  $n_\pm = d(N_+ + N_-)/dE$  of  $DM^0$  and  $(DM^+ + DM^-)$ . They read:<sup>6</sup>

$$\frac{dn_0(\ell, E)}{d\ell} = +\frac{M}{E} \frac{n_\pm(E)}{\tau} + N_N \left[ -n_0(E) \sigma_{CC}(E) + \frac{1}{2} \int_E^\infty dE' n_\pm(E') \frac{d\sigma_{CC}(E', E)}{dE} \right], \quad (26a)$$

<sup>5</sup>Supersymmetric models with gravitino LSP may have a long-lived, charged next-to-lightest particle that behaves in a way qualitatively similar to MDM [21]. Furthermore, fermionic MDM with  $n = 3$  and  $Y = 0$  arises in supersymmetry in the limit of pure-wino lightest supersymmetric particle.

<sup>6</sup>Similar equations have been of course used in the analogous problem for neutrinos [19] and for high energy neutralinos [20].

$$\begin{aligned} \frac{dn_{\pm}(\ell, E)}{d\ell} &= -\frac{M}{E} \frac{n_{\pm}(E)}{\tau} + N_N \left[ -\frac{1}{2} n_{\pm}(E) \sigma_{\text{CC}}(E) + \int_E^{\infty} dE' n_0(E') \frac{d\sigma_{\text{CC}}(E', E)}{dE} \right] + \\ &\quad -\frac{d}{dE} \left( n_{\pm} \frac{dE_{\text{loss}}}{d\ell} \right), \end{aligned} \quad (26b)$$

where  $N_N(\ell)$  is the number density profile of nucleons in the Earth [22], and  $E$  is the DM energy. The first terms account for  $\text{DM}^{\pm}$  decays. The integro-differential terms within square brackets account for  $\text{DM}^0 \leftrightarrow \text{DM}^{\pm}$  CC scatterings. The last term accounts for the energy losses undergone by  $\text{DM}^{\pm}$ , due to electromagnetic and Neutral Current (NC) scatterings:

$$\frac{dE_{\text{loss}}}{d\ell} = \frac{dE_{\text{loss,em}}}{d\ell} + \frac{dE_{\text{loss,NC}}}{d\ell}. \quad (27)$$

We will later verify that the NC energy losses are subdominant and can be approximated as continuous, like electromagnetic energy losses.

The cross section for the CC partonic scatterings  $\text{DM}^0 d \rightarrow \text{DM}^- u$ ,  $\text{DM}^0 \bar{d} \rightarrow \text{DM}^+ \bar{u}$ ,  $\text{DM}^0 u \rightarrow \text{DM}^+ d$  and  $\text{DM}^0 \bar{u} \rightarrow \text{DM}^- d$  are all given by, for fermionic MDM:

$$\frac{d\hat{\sigma}_{\text{CC}}}{d\hat{t}} = \left( \frac{E}{(\hat{s} - M^2)} \frac{d\hat{\sigma}_{\text{CC}}}{dE} \right) \frac{g_2^4(n^2 - 1)}{256\pi} \frac{2M^4 + 2\hat{s}^2 + 2\hat{s}\hat{t} + \hat{t}^2 - 4M^2(\hat{s} + \hat{t})}{(\hat{s} - M^2)^2(\hat{t} - M_W^2)^2} \quad (28)$$

where  $\hat{s}$  and  $\hat{t}$  are the usual partonic Mandelstam variables. The total cross section for  $\text{DM}^0 N \rightarrow \text{DM}^+ N'$ ,  $\text{DM}^- N'$  is

$$\sigma_{\text{CC}}(s) = \int_0^1 dx q(x) \int_{-(\hat{s}-M^2)^2/\hat{s}}^0 d\hat{t} \frac{d\hat{\sigma}}{d\hat{t}}, \quad (29)$$

where  $q(x)$  is the parton distribution function [23], summed over all quarks and anti-quarks. We here approximated the neutron/proton fraction in Earth matter as unity. The nucleon  $N$  is at rest with mass  $m_N$ , and  $\text{DM}^0$  has energy  $E_0$ , so that  $s = M^2 + 2m_N E_0$  and  $\hat{s} = M^2 + 2xm_N E_0$ . A similar expression holds for NC scatterings of  $\text{DM}^{\pm}$  particles  $\text{DM}^{\pm} q \rightarrow \text{DM}^{\pm} q$  (whereas  $\text{DM}^0$  has no NC interactions due to  $Y = 0$ ):

$$\frac{d\hat{\sigma}_{\text{NC}}}{d\hat{t}} = \frac{g_2^4(g_{Lq}^2 + g_{Rq}^2)}{16\pi} \frac{2M^4 + 2\hat{s}^2 + 2\hat{s}\hat{t} + \hat{t}^2 - 4M^2(\hat{s} + \hat{t})}{(\hat{s} - M^2)^2(\hat{t} - M_Z^2)^2} \quad (30)$$

where  $g_{Lq} = T_{3q} - Q_q s_W^2$ ,  $g_{Rq} = -Q_q s_W^2$  and  $q$  denotes any quark or anti-quark. The same cross sections, up to terms suppressed by powers of  $M_{W,Z}/M$ , hold for scalar MDM.

In fig. 7a we plot the MDM total CC cross section. We can understand its main features as follows. The total partonic cross section approximatively is

$$\hat{\sigma}_{\text{CC}} \simeq \frac{g_2^4(n^2 - 1)}{128\pi M_W^2} \cdot \begin{cases} 2(xE/E_*)^2 & \text{at } xE \ll E_* \\ 1 & \text{at } xE \gg E_* \end{cases} \quad (31)$$

where  $E_* \equiv MM_W/m_N \sim 10^{15}$  eV (the transition between the two regimes happens when  $t \sim -M_W^2$ ). Therefore one has a constant  $\hat{\sigma}_{\text{CC}} \approx 10^{-33} \text{cm}^2$  at  $xE \gg E_*$ . Upon integration over the parton densities, the nucleonic  $\sigma_{\text{CC}}$  becomes a slowly growing function of  $E$  because at higher  $E$  partons with smaller  $x \gtrsim E_*/E$  contribute, and  $q(x)$  grows as  $x \rightarrow 0$ . This is analogous to what happens for neutrinos [24]. Indeed, at high energies, the MDM CC cross section in fig. 7 approaches the dotted red line of the analogous result for  $\nu_{\mu,\tau}$ .



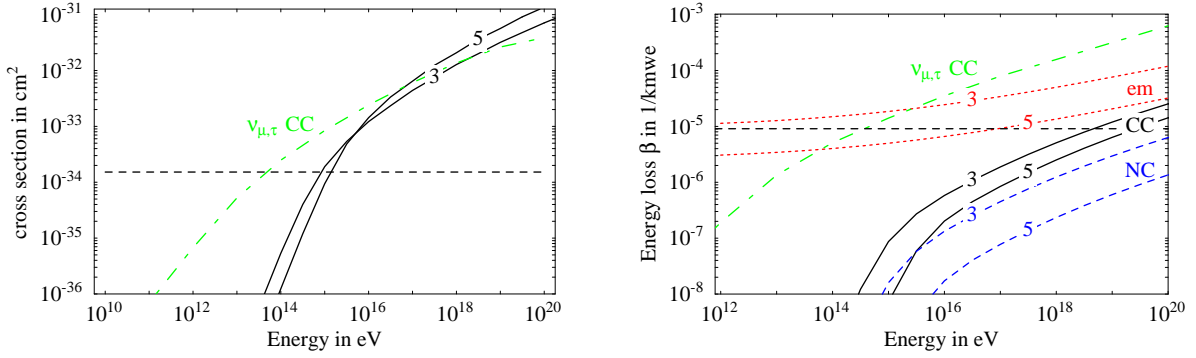


Figure 7: *Left plot: CC cross section for fermionic MDM (black solid) with  $n = 3, 5$  on nucleons. The same cross section for neutrinos (green dot-dashed) is reported for comparison. Right plot: average energy loss parameters  $\beta = -d \ln E / d\ell$  due to CC interactions (black solid lines), NC interactions (blue dashed), and electromagnetic interactions (red dotted). For comparison, the green dot-dashed line show the CC energy loss of  $\nu_{\mu, \tau}$ . The horizontal lines show the thickness of the Earth, crossed vertically.*

For the electromagnetic energy losses of  $DM^\pm$  one has the standard parameterization [25]

$$-\frac{dE_{\text{loss, em}}}{d\ell} = \alpha + \beta_{\text{em}} E \quad (32)$$

where  $\alpha \approx 0.24 \text{ TeV/kmwe}$  approximates the energy loss due to ionization effects [25] and the  $\beta_{\text{em}}$  term accounts for the radiative losses: it receives contributions from bremsstrahlung,  $e^+e^-$  pair production and photonuclear scattering (i.e. inelastic electromagnetic collisions on nuclei). The latter two effects have comparable importance, while bremsstrahlung is subdominant for a very heavy particle such as MDM [26]. We follow the approach of [26] and adopt a parameterization for  $\beta_{\text{em}}$  with a mild dependance on the energy:

$$\beta_{\text{em}} \simeq 2.5 \cdot 10^{-5} \frac{1}{\text{kmwe}} \frac{\text{TeV}}{M} \left[ 1 + \left( \frac{E}{10^{15} \text{ eV}} \right)^{0.215} \right]. \quad (33)$$

Before proceeding to the numerical solution of the equations in (26), we can gain understanding on the expected results by simplifying the treatment of the CC energy losses. In analogy with the standard parameterization, we can define an average energy loss suffered by  $DM^0$  particles due to CC interactions as

$$-\beta_{\text{CC}}(E) = \frac{1}{E} \frac{dE_{\text{loss, CC}}}{d\ell} = N_N \int_0^1 dx q(x) \int_{-(\hat{s}-M^2)^2/\hat{s}}^0 d\hat{t} \frac{\hat{t}}{\hat{s}-M^2} \frac{d\hat{\sigma}_{\text{CC}}}{d\hat{t}}. \quad (34)$$

A completely analogous expression holds for  $\beta_{\text{NC}} = -1/E dE_{\text{loss, NC}}/d\ell$ . Both are plotted in fig. 7b, in units of  $1/\text{kmwe} = 10^{-5} \text{ cm}^2/\text{gram}$ . The horizontal line indicates the value above which a particle loses a significant amount of energy while vertically crossing the Earth (its thickness being  $1.1 \cdot 10^5 \text{ kmwe}$ ). Energy losses can be understood analogously to the total cross section, and are dominated by partons with  $xE \sim E_*$ . Parton distributions have been measured

at  $x \gtrsim 10^{-4}$  and theoretical extrapolations to smaller  $x$  can have  $\mathcal{O}(1)$  uncertainties, that affect our results.

The fraction of energy lost in one scattering is small,  $\sim \beta/N_N\sigma \lesssim 10^{-2}$  at the UHE energies that will be relevant for us, so that all energy losses can be approximated as continuous.<sup>7</sup>

$$-\frac{dE_0}{d\ell} = \beta_{\text{CC}}E_0, \quad -\frac{dE_{\pm}}{d\ell} = \alpha + \left(\frac{\beta_{\text{CC}}}{2} + \beta_{\text{em}} + \beta_{\text{NC}}\right)E_{\pm} \quad (35)$$

where  $E_0$  ( $E_{\pm}$ ) is the energy of  $\text{DM}^0$  ( $\text{DM}^{\pm}$ ). Therefore, we do not need to study the evolution of the DM energy spectrum (dictated by eq. (26)) but we just need to follow how any initial energy decreases while crossing the Earth. This process is well approximated by the following system of two ordinary differential equations:

$$\frac{dN_0}{d\ell} = -N_N\sigma_{\text{CC}}N_0 + \frac{1 - N_0}{1/\tau + 1/N_N\sigma_{\text{CC}}} \quad (36a)$$

$$\frac{dE}{d\ell} = N_0\frac{dE_0}{d\ell} + (1 - N_0)\frac{dE_{\pm}}{d\ell}. \quad (36b)$$

where  $0 \leq N_0 \leq 1$  is the fraction of DM present in neutral state, and  $1 - N_0$  is the fraction of DM present in charged state. The initial conditions are  $N_0(0) = 1$  and  $E(0) = E_{\text{in}}$ .

Fig. 8a shows the numerical relevance of the various effects, and allows to understand their interplay. The  $\text{DM}^0$  interaction length starts to be smaller than the Earth thickness at  $E \gtrsim 10^{15}$  eV, but these interactions have no effects, since the produced  $\text{DM}^{\pm}$  regenerates  $\text{DM}^0$  in a negligible length and with negligible energy losses. At  $E \gtrsim 10^{18}$  eV energy losses start to be moderately relevant, and at roughly the same energy the  $\text{DM}^{0,\pm}$  mean free-path in Earth matter becomes comparable to the  $\text{DM}^{\pm}$  decay length: the Earth is crossed losing an order one fraction of the initial energy, and spending an order one fraction of the path as  $\text{DM}^{\pm}$  rather than as  $\text{DM}^0$ .

Fig. 8b shows the numerical results: the black continuous line shows the  $\text{DM}^{\pm}$  fraction  $1 - N_0$  as function of the initial energy, after vertically crossing the Earth. The dashed line shows the same fraction as function of the final energy. Actually, we have two dashed lines obtained by solving the full and simplified system of evolution equations: their agreement confirms the validity of the continuum energy loss approximation. (In the full case we assumed an initial  $\text{DM}^0$  energy spectrum proportional to the CR energy spectrum). These  $\text{DM}^{\pm}$  fraction is roughly given by  $1 - N_0 \approx (1 + N_N\sigma_{\text{CC}}/\tau)^{-1}$ , and depends on the local nucleon density  $N_N$ , averaged over a typical scale of tens of km. This figure allows to compute the  $\text{DM}^{\pm}$  rate for any initial energy spectrum of DM. The upper red dot-dashed line shows the ratio  $E_{\text{out}}/E_{\text{in}}$  between the final and initial energy.

Fig. 9 shows the analogous result for the fermion 5-plet, which has a  $\text{DM}^{\pm\pm}$  component with a much shorter life-time  $\approx 0.05$  cm. Due to its fast decay, the new  $\text{DM}^{\pm\pm}$  component is not present with a significant abundance at the UHE CR energies  $E \lesssim 10^{20}$  eV.

## 5.2 Production of UHE Minimal Dark Matter

Minimal DM particles may exist at ultra high energies if they are a component of the primary cosmic rays, if they manage to be produced by standard UHE CR in the earth's atmosphere

---

<sup>7</sup>The fraction of energy lost in one  $\text{DM}^{\pm} \rightarrow \text{DM}^0$  decay is  $\Delta M/M \sim 10^{-4}$  and can be neglected.

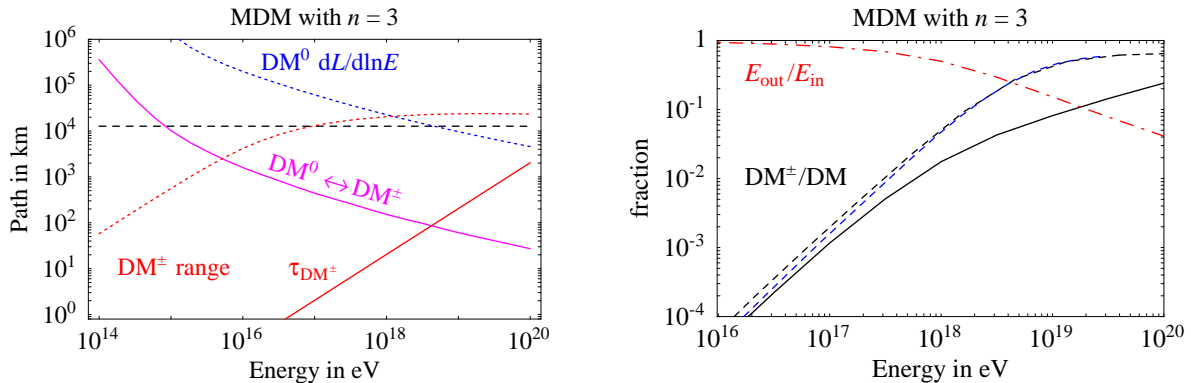


Figure 8: We consider the wino-like MDM: a fermion with  $n = 3$  and  $M = 2.7$  TeV. **Left plot:** The dotted lines show the length scales that characterize energy losses in matter with  $\rho = 6.3 \text{ g/cm}^3$ . More precisely: with the upper blue dotted line we show the effective  $1/\beta_{CC}$  experienced by a  $DM^0$  as if it never transformed in the charged state, and with the red dotted line the range of a stable  $DM^\pm$ . The solid lines show the effects of neutral to charge transformations and vice-versa: the solid ascending red line is the  $DM^\pm$  life-time while the solid descending pink line is the mean free path for  $DM^0 \rightarrow DM^\pm$  CC interactions. **Right plot:** we consider a  $DM^0$  which crosses the Earth vertically with initial energy  $E_{in}$  and we show  $E_{out}/E_{in}$  (upper red dot-dashed line) and the fraction of  $DM^\pm$  over the total number of DM particles ( $DM^0 + DM^\pm$ ). These fractions are shown as a function of  $E_{out}$  in the simplified numerical approach (black dashed line) and in the full numerical approach (blue dashed line, almost superimposed to the former) as well as a function of  $E_{in}$  (black solid line).

or if more exotic CR scenarios will prove to be motivated. Let us look at these opportunities in turn.

Although the mechanism that accelerates the UHE primary CR has not yet been established, the plausible astrophysical standard mechanism (first-order Fermi acceleration in magnetic shock waves around various objects, such as gamma-ray bursts and supernova remnants) accelerates stable charged particles. In the MDM scenario, the neutral  $DM^0$  is accompanied by a charged partner with life-time  $\tau \sim \text{cm}$ : this value is not macroscopic enough to lead to acceleration of  $DM^\pm$  particles. Moreover, the standard mechanism accelerates protons or charged nuclei in regions that are believed to be transparent: i.e. the local density is so small these primary CR particles negligibly hit on the surrounding DM accelerating it, or on the surrounding material producing DM pairs.

Production of DM pairs might be relevant when UHE CR particles hit the Earth. The number of DM particles generated by one UHE proton with energy  $E \gtrsim (2M)^2/m_p \sim 10^{18}$  eV (which is the energy range that leads to a sizable  $DM^\pm$  fraction) is  $r \sim \sigma/\sigma_{pp} \sim 10^{-11}$ , where  $\sigma_{pp} \sim 1/m_\pi^2$  is the total hadronic cross section, and  $\sigma$  is the  $pp \rightarrow DM DM$  cross section, computed in [6]. A UHE electron neutrino produces a higher fraction of DM,  $r \sim \sigma/\sigma_\nu \sim 10^{-6}$ , but only at higher energies  $E \gtrsim (2M)^2/m_e$ . These processes lead to a double DM signature, but their rate looks too small for present detectors (see e.g. [20, 26]). A UHE DM rate detectable in forthcoming experiments can arise in more speculative scenarios: e.g. they may be a component of the UHE CR generated by decays of ultra-heavy particle, in the so called ‘top-down’ scenarios [27].

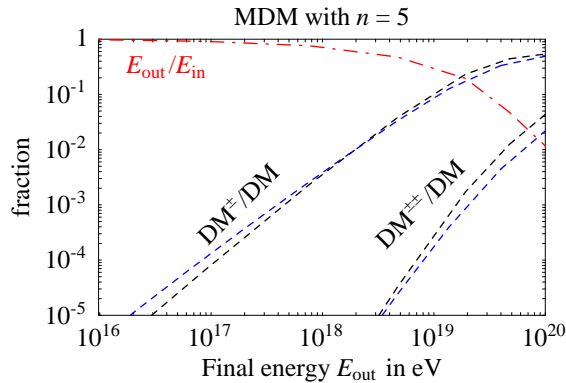


Figure 9: We consider the MDM fermion with  $n = 5$  and  $M = 10$  TeV which crosses the earth vertically with initial energy  $E_{\text{in}}$  and final energy  $E_{\text{out}}$ . We show  $E_{\text{out}}/E_{\text{in}}$  (upper red dot-dashed line) and the fraction of  $\text{DM}^{\pm}$  and of  $\text{DM}^{\pm\pm}$  over the total number of DM particles as function of  $E_{\text{out}}$ .

In terms of absolute numbers, if DM constitutes a number fraction  $r$  of CR with energy above  $10^{17}$  eV ( $10^{18}$  eV), one expects a flux of  $\approx 60r$  ( $\approx 6r$ )  $\text{DM}^{\pm}$  per  $\text{km}^2 \cdot \text{yr}$ , in the case  $n = 3$ . Atmospheric neutrinos generate a flux of  $\approx 10^3$  ( $\approx 10$ ) up-going muons per  $\text{km}^2 \cdot \text{yr}$  with  $E > 10^{13}$  eV ( $10^{14}$  eV): as discussed in the next section, this is a background to  $\text{DM}^{\pm}$  searches.

### 5.3 Detection of UHE $\text{DM}^{\pm}$

Let us study how UHE  $\text{DM}^{\pm}$  can be searched for. In a detector like IceCUBE or Antares  $\text{DM}^{\pm}$  roughly look like muons with fake energy  $E_{\mu} = E_{\pm}\beta_{\text{CC}}/\beta_{\mu} \sim 10^{-4}E_{\pm}$ , because muon energy losses are approximatively given by  $-dE_{\mu}/d\ell = \alpha + \beta_{\mu}E_{\mu}$  with  $\beta_{\mu} \approx 0.2/\text{kmwe}$  [25]: indeed  $\beta$  is roughly inversely proportional to the particle mass.

One therefore needs to carefully study charged tracks to see the difference between a  $\text{DM}^{\pm}$  with  $E_{\pm} \sim 10^{18}$  eV and a muon with  $E_{\mu} \sim 10^{14}$  eV. The muon would loose all its energy in about 2 kmwe (with a characteristic energy loss profile) while  $\text{DM}^{\pm}$  have a much longer range in matter. On the contrary, the muon is essentially stable, while  $\text{DM}^{\pm}$  decays in about 10 km (less at lower energy: see fig. 8a), suddenly disappearing into a  $\text{DM}^0$  and a  $\pi^{\pm}$  with energy  $E_{\pi} \sim m_{\pi}E_{\pm}/M$ . Furthermore, the characteristic scale for the  $\text{DM}^0 \leftrightarrow \text{DM}^{\pm}$  transformation is about tens of km. Unfortunately it seems very difficult to exploit these differences to discriminate between a  $\mu^{\pm}$  and a  $\text{DM}^{\pm}$  in the forthcoming IceCUBE km-size detector [18], because it only has a 1 km size and modest granularity.

## 6 Conclusions

We considered DM that fills one  $\text{SU}(2)$  multiplet and only interacts with SM vectors (‘Minimal Dark Matter’ [6]). This model has one free parameter, the DM mass  $M$ , which is fixed from the observed DM abundance assuming that DM is a thermal relic. We have reconsidered this computation including non-perturbative corrections due to Coulomb-like forces mediated by SM vectors, that significantly increase  $M$ . For example, a fermion 5-plet automatically behaves as MDM (and in particular is automatically stable): its mass increases from  $M = 4.4$  TeV [6] to

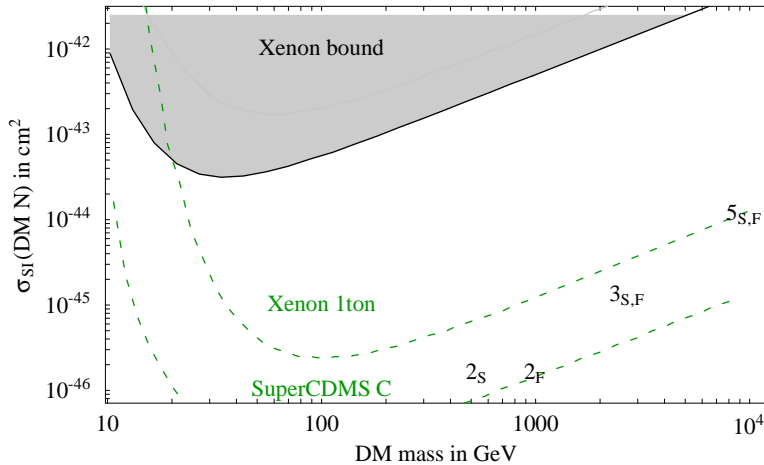


Figure 10: Predicted mass and predicted spin-independent cross sections per nucleon of MDM candidates. Scalar (Fermionic) SU(2)  $n$ -tuplets are denoted as  $n_S$  ( $n_F$ ). The shaded region is excluded by [13] and the dashed lines indicate the planned sensitivity of future experiments [28]. The prediction for doublets with  $Y \neq 0$  hypercharge holds up to the caveats discussed in the text; furthermore we assumed the nuclear matrix element  $f = 1/3$  and the Higgs mass  $m_h = 115$  GeV.

10 TeV. The cosmological freeze-out abundance is plotted as function of  $M$  in fig. 4a (fermion 5-plet), 2a (wino-like fermion 3-plet,  $M \approx 2.7$  TeV [7]), 3a (scalar 3-plet,  $M \approx 2.5$  TeV) and 5a (Higgsino-like fermion 2-plet,  $M \approx 1.0$  TeV). We also discussed the scalar 5-plet ( $M \approx 9.4$  TeV) and 7-plet ( $M \approx 25$  TeV).

Having fixed  $M$ , we studied the MDM signals.

At colliders, the charged components  $DM^\pm$  in the MDM multiplet manifest as non-relativistic cm-scale ionizing charged tracks negligibly bent by the  $B \sim$  Tesla magnetic field present around the interaction region.  $DM^\pm$  decays with 97.7% branching ratio into  $\pi^\pm$  [6] (see also [29]), giving a relativistic track bent by the magnetic fields. Everything happens in the inner portion of the detector and this signature is free from SM backgrounds. However, at a hadron collider like LHC it seems not possible to trigger on this signature: level-1 triggers are located far from the interaction point and MDM candidates are so heavy that the event rate is too low. Unlike in other scenarios we cannot choose a favorable benchmark point in a vast parameter space.

Astrophysics offers more promising detection prospects.

The cross section for *direct DM detection* negligibly depends on  $M$ , and remains the same as in [6]: fig. 10 summarizes the situation. Since MDM is much heavier than a typical nucleus, direct DM searches can precisely reconstruct only the combination  $\sigma_{SI}/M$ .

Next, we considered *indirect DM detection*, computing how non-perturbative effects enhance the  $DM^0 DM^0$  annihilations into  $W^+W^-$ ,  $\gamma\gamma$ ,  $\gamma Z$ ,  $ZZ$ . Results are shown in fig. 2b (wino-like fermion 3-plet [10]), 3b (scalar 3-plet), 4b (5-plet), and 5b (Higgsino-like fermion 2-plet [10]). Signal rates can now be computed by combining this particle physics with (uncertain) astrophysics: for example fig. 6 shows the predicted spectrum of galactic  $\gamma$ .

Finally, we assumed that some DM particles are present among the cosmic rays at Ultra High Energies and identified an unusual signal, characteristic of heavy and quasi-degenerate multiplets containing neutral and charged components: a  $DM^0$  crosses the Earth without losing

much energy and, at  $E \gtrsim 10^{17}$  eV, a sizable fraction of the travel is done as  $\text{DM}^\pm$ , leading to charged tracks, that might be detectable in neutrino telescopes such as IceCUBE. Figs 8 and 9 quantitatively show how frequent this phenomenon is.

**Acknowledgements** We thank Masato Senami for several clarifications about [7]. We also thank Gianfranco Bertone, Jürgen Brunner, Giacomo Cacciapaglia, Paschal Coyle, Michele Frigerio, Dario Grasso, John Gunion, T. Montaruli, Slava Rychkov, Günter Sigl, Igor Sokalski and Igor Tkachev for useful discussions. The work of M.C. is supported in part by INFN under the postdoctoral grant 11067/05 and in part by CEA/Saclay.

## A Annihilation cross sections

We here give results for the tree-level DM DM annihilation cross sections. We define the adimensional ‘reduced cross section’

$$\hat{\sigma}(s) = \int_{-s}^0 dt \sum \frac{|\mathcal{A}|^2}{8\pi s} \quad (37)$$

where  $s, t$  are the Madelstam variables and the sum runs over all DM components and over all SM vectors, fermions and scalars, assuming that all SM masses are negligibly small.

The DM abundance is computed by solving the Boltzmann equation

$$sZH z \frac{dY}{dz} = -2 \left( \frac{Y^2}{Y_{\text{eq}}^2} - 1 \right) \gamma_A, \quad \gamma_A = \frac{T}{64\pi^4} \int_{4M^2}^{\infty} ds s^{1/2} K_1 \left( \frac{\sqrt{s}}{T} \right) \hat{\sigma}_A(s) \quad (38)$$

where  $z = M/T$ ,  $K_1$  is a Bessel function,  $Z = (1 - \frac{1}{3} \frac{z}{g_s} \frac{dg_s}{dz})^{-1}$ , the entropy density of SM particles is  $s = 2\pi^2 g_{*s} T^3 / 45$ ,  $Y = n_{\text{DM}}/s$  where  $n_{\text{DM}}$  is the number density of DM particles plus anti-particles, and  $Y_{\text{eq}}$  is the value that  $Y$  would have in thermal equilibrium. We can write a single equation for the total DM density because DM scatterings with SM particles maintain thermal equilibrium within and between the single components. We ignored the Bose-Einstein and Fermi-Dirac factors as they are negligible at the temperature  $T \sim M/26$  relevant for DM freeze-out.

We assume that DM fills one  $\text{SU}(2)$  multiplet with dimension  $n$  and hypercharge  $Y$ ; when  $Y \neq 0$  the conjugate multiplet is also added in order to allow for a gauge-invariant DM mass term. For example, the Higgsino has  $n = 2$  and  $Y = 1/2$ ; the wino has  $n = 3$  and  $Y = 0$ . We define  $g_{\mathcal{X}}$  as the number of DM degrees of freedom:  $g_{\mathcal{X}} = n$  for scalar DM with  $Y = 0$ ;  $g_{\mathcal{X}} = 2n$  for scalar DM with  $Y \neq 0$  and for spin-1/2 (Majorana) DM with  $Y = 0$ ;  $g_{\mathcal{X}} = 4n$  for spin-1/2 (Dirac) DM with  $Y \neq 0$ . For fermion DM we get

$$\begin{aligned} \hat{\sigma}_A &= \frac{g_{\mathcal{X}}}{24\pi n} \left[ (9C_2 - 21C_1)\beta + (11C_1 - 5C_2)\beta^3 - 3 \left( 2C_1(\beta^2 - 2) + C_2(\beta^2 - 1)^2 \right) \ln \frac{1 + \beta}{1 - \beta} \right] \\ &+ g_{\mathcal{X}} \left( \frac{3g_2^4(n^2 - 1) + 20g_Y^4 Y^2}{16\pi} + \frac{g_2^4(n^2 - 1) + 4g_Y^4 Y^2}{128\pi} \right) \left( \beta - \frac{\beta^3}{3} \right) \end{aligned} \quad (39)$$

and for scalar DM we get

$$\begin{aligned} \hat{\sigma}_A &= \frac{g_{\mathcal{X}}}{24\pi n} \left[ (15C_1 - 3C_2)\beta + (5C_2 - 11C_1)\beta^3 + 3(\beta^2 - 1) \left( 2C_1 + C_2(\beta^2 - 1) \right) \ln \frac{1 + \beta}{1 - \beta} \right] \\ &+ g_{\mathcal{X}} \left( \frac{3g_2^4(n^2 - 1) + 20g_Y^4 Y^2}{48\pi} + \frac{g_2^4(n^2 - 1) + 4g_Y^4 Y^2}{384\pi} \right) \cdot \beta^3 \end{aligned} \quad (40)$$

where  $x = s/M^2$  and  $\beta = \sqrt{1 - 4/x}$  is the DM velocity in the DM DM center-of-mass frame. The first line gives the contribution of annihilation into vectors, the second line contains the sum of the contributions of annihilations into SM fermions and vectors respectively. The gauge group factors are defined as

$$C_1 = \sum_{A,B} \text{Tr} T^A T^A T^B T^B = g_Y^4 n Y^4 + g_2^2 g_Y^2 Y^2 \frac{n(n^2 - 1)}{2} + g_2^4 \frac{n(n^2 - 1)^2}{16} \quad (41)$$

$$C_2 = \sum_{A,B} \text{Tr} T^A T^B T^A T^B = g_Y^4 n Y^4 + g_2^2 g_Y^2 Y^2 \frac{n(n^2 - 1)}{2} + g_2^4 \frac{n(n^2 - 1)(n^2 - 5)}{16} \quad (42)$$

where the sum is over all SM vectors  $A = \{Y, W^1, W^2, W^3\}$  with gauge coupling generators  $T^A$ .

The DM freeze-out abundance is accurately determined by the leading two terms of the expansion of for small  $\beta$ , that describe the  $s$ -wave and the  $p$ -wave contributions. This approximation allows to analytically do the thermal average in eq. (38):

$$\hat{\sigma}_A \stackrel{\beta \rightarrow 0}{\simeq} c_s \beta + c_p \beta^3 + \dots \quad \text{implies} \quad \gamma_A \stackrel{\beta \rightarrow 0}{\simeq} \frac{MT^3 e^{-2M/T}}{32\pi^3} \left[ c_s + \frac{3T}{2M} (c_p + \frac{c_s}{2}) + \dots \right]. \quad (43)$$

More complex models of DM can have extra interactions beyond gauge interactions, but the gauge contribution we computed accurately is the minimal model-independent contribution present in all cases. Eq. (38) also arises as a subset of the Boltzmann equations that describe leptogenesis from decays of gauge-interacting particles: the scalar triplet corresponds to  $n = 3$ ,  $Y = 1$  [30], and the fermion triplet to  $n = 3$  and  $Y = 0$  [31].

## References

- [1] See G. Bertone, D. Hooper and J. Silk, Phys. Rept. 405 (2005) 279 [[hep-ph/0404175](#)] for a recent review.
- [2] These numbers conservatively summarize various recent global analyses of cosmological data within the  $\Lambda$ CDM model that found compatible values and uncertainties: D. N. Spergel *et al.* [WMAP collaboration], [astro-ph/0603449](#), M. Cirelli and A. Strumia, JCAP 0612 (2006) 013 [[astro-ph/0607086](#)], M. Tegmark *et al.*, Phys. Rev. D74 (2006) 123507 [[astro-ph/0608632](#)].
- [3] A. Gould *et al.*, Phys. Lett. B238 (1990) 337.
- [4] Strongly interacting, “hadronized”, Dark Matter is subject to a number of constraints analysed in G. D. Starkman, A. Gould, R. Esmailzadeh and S. Dimopoulos, Phys. Rev. D41 (1990) 3594 that leave only implausible windows open. Recently, G. D. Mack, J. F. Beacom and G. Bertone, [0705.4298](#) went in the direction of closing those windows to safeguard Earth’s heat flow.
- [5] The upper bound is imposed by the null results of direct detection searches, see [[13](#)]. See also G. Belanger, A. Pukhov and G. Servant, [0706.0526](#) for a recent analysis of this feature as a phenomenological assumption and in specific models.
- [6] M. Cirelli, N. Fornengo, A. Strumia, Nucl. Phys. B753 (2006) 178 [[hep-ph/0512090](#)].
- [7] The relevance of non-perturbative electroweak corrections to DM freeze-out was pointed out in J. Hisano, S. Matsumoto, M. Nagai, O. Saito, M. Senami, Phys. Lett. B646 (2007) 34 [[hep-ph/0610249](#)]. Non-perturbative QCD corrections were considered in H. Baer, K. Cheung, J. Gunion, Phys. Rev. D59 (1999) 075002 [[hep-ph/9806361](#)].
- [8] R. Barbieri, L. Hall, V. Rychkov, Phys. Rev. D74 (2006) 015007 [[hep-ph/0603188](#)]. A. Pierce, J. Thaler, [hep-ph/0703056](#). F. D’Eramo, [0705.4493](#). L. Lopez Honorez, E. Nezri, J. F. Oliver and M. H. G. Tytgat, JCAP 0702 (2007) 028 [[hep-ph/0612275](#)], R. Enberg, P. Fox, L. Hall, A. Papaioannou, M. Papucci, [0706.0918](#).
- [9] A. Sommerfeld, Ann. Phys. 11 257 (1931).
- [10] J. Hisano, S. Matsumoto, M. M. Nojiri and O. Saito, Phys. Rev. D 71 (2005) 015007 [[hep-ph/0407168](#)]. J. Hisano, S. Matsumoto and M. M. Nojiri, Phys. Rev. D 67 (2003) 075014 [[hep-ph/0212022](#)]. J. Hisano, S. Matsumoto and

- M. M. Nojiri, Phys. Rev. Lett. 92 (2004) 031303 [hep-ph/0307216]. J. Hisano, S. Matsumoto, M. M. Nojiri and O. Saito, Phys. Rev. D 71 (2005) 063528 [hep-ph/0412403]. J. Hisano, S. Matsumoto, O. Saito, M. Senami, Phys. Rev. D73 (2006) 055004 [hep-ph/0511118].
- [11] An approximated discussion of the SM potential at finite temperature can be found in M. Dine, R. Leigh, P. Huet, A. Linde, D. Linde, Phys. Rev. D46 (1992) 550 [hep-ph/9203203].
- [12] D. J. Gross, R. D. Pisarski and L. G. Yaffe, Rev. Mod. Phys. 53, 43 (1981). H. Weldon, Phys. Rev. D26 (1982) 1394.
- [13] Xenon-10 collaboration, 0706.0039.
- [14] H.E.S.S. collaboration, Nature 439 (2006) 695 [astro-ph/0603021]. See L. Bergstrom, T. Bringmann, M. Eriksson, M. Gustafsson, AIP Conf. Proc. 861 (2006) 814 [astro-ph/0609510] for a recent summary of  $\gamma$ -line signals of some DM candidates.
- [15] L. Bergstrom, P. Ullio, J. Buckley, Astropart. Phys. 9 (1998) 137 [astro-ph/9712318].
- [16] J. Navarro, C. Frenk, S. White, Astrophys. J. 462 (1996) 563 [astro-ph/9508025].
- [17] The ANTARES collaboration, “A Deep Sea Telescope for High Energy Neutrinos - Proposal for a 0.1km<sup>2</sup> Neutrino Telescope”, 31 May 1999, web site [antares.in2p3.fr](http://antares.in2p3.fr).
- [18] IceCube collaboration, AIP Conf. Proc. 842 (2006) 971 [astro-ph/0601269].
- [19] S. Iyer, M. H. Reno and I. Sarcevic, Phys. Rev. D61 (2000) 053003 [hep-ph/9909393]. S. I. Dutta, M. H. Reno and I. Sarcevic, Phys. Rev. D62 (2000) 123001 [hep-ph/0005310]. A. L’Abbate, T. Montaruli, I. Sokalski, Astropart. Phys. 23 (2005) 57 [hep-ph/0406133]. For a summary of the formalism, including the effect of oscillations relevant at sub-TeV energies, see M. Cirelli, N. Fornengo, T. Montaruli, I. Sokalski, A. Strumia and F. Vissani, Nucl. Phys. B727 (2005) 99 [hep-ph/0506298].
- [20] S. Bornhauser and M. Drees, Astropart. Phys. 27 (2007) 30 [hep-ph/0603162].
- [21] I. Albuquerque, G. Burdman and Z. Chacko, Phys. Rev. Lett. 92 (2004) 221802 [hep-ph/0312197]. M. Ahlers, J. Kersten and A. Ringwald, JCAP 0607 (2006) 005 [hep-ph/0604188]. I. F. M. Albuquerque, G. Burdman and Z. Chacko, Phys. Rev. D75 (2007) 035006 [hep-ph/0605120]. M. Ahlers, J. I. Illana, M. Masip and D. Meloni, 0705.3782.
- [22] A.M. Dziewonski, D.L. Anderson, Phys. Earth Planet. Interior 25 (1981) 297. See also [mahi.ucsd.edu/Gabi/rem.html](http://mahi.ucsd.edu/Gabi/rem.html).
- [23] We use the parton distribution functions from S. Alekhin, JETP Lett. 82 (2005) 628 [hep-ph/0508248] that are available in Mathematica format from [sirius.ihep.su/~alekhin/pdfa02](http://sirius.ihep.su/~alekhin/pdfa02) and extend down to small  $x \sim 10^{-7}$ , as needed for the computation of nucleonic cross sections at UHE.
- [24] For a review and references, see section 4.3 of A. Strumia and F. Vissani, hep-ph/0606054.
- [25] P. H. Barrett, L. M. Bollinger, G. Cocconi, Y. Eisenberg and K. Greisen, Rev. Mod. Phys. 24 (1952) 133. D. E. Groom, N. V. Mokhov and S. I. Striganov, Atomic Data and Nuclear Tables 78 (2001) 183-356.
- [26] M. H. Reno, I. Sarcevic and S. Su, Astropart. Phys. 24 (2005) 107 [hep-ph/0503030].
- [27] V. Berezhinsky, M. Kachelriess, A. Vilenkin, Phys. Rev. Lett. 79 (1997) 4302 [astro-ph/9708217].
- [28] For the Xenon project see E. Aprile *et al.*, Nucl. Phys. Proc. Suppl. 138 (156) 2005 [astro-ph/0407575]. For the SuperCDMS project see CDMS-II collaboration, eConf C041213 (2004) 2529 [astro-ph/0503583]. Useful comparisons can be done using the tools in [dendera.berkeley.edu/plotter/entryform.html](http://dendera.berkeley.edu/plotter/entryform.html).
- [29] J. Gunion, S. Mrenna, Phys. Rev. D62 (2000) 015002 [hep-ph/9906270].
- [30] T. Hambye, M. Raidal, A. Strumia, Phys. Lett. B632 (2006) 667 [hep-ph/0510008].
- [31] T. Hambye, Y. Lin, A. Notari, M. Papucci, A. Strumia, Nucl. Phys. B695 (2004) 169 [hep-ph/0312203]. Their cross section into gauge bosons should be increased by a factor 2, and this has a minor effect on the baryon asymmetry.